Published in final edited form as:
J Neurosci Methods. 2008 June 30; 171(2): 197–206.

A System for Studying Facial Nerve Function in Rats through Simultaneous Bilateral Monitoring of Eyelid and Whisker Movements

James T. Heaton, Ph.D.[1], **Jeffrey M. Kowaleski, B.S.**[2], **Roberto Bermejo, Ph.D.**[3], **H. Philip Zeigler, Ph.D.**[3], **David J. Ahlgren, Ph.D.**[4], and **Tessa A. Hadlock, M.D.**[2]

1*Department of Surgery, Harvard Medical School, Massachusetts General Hospital, Boston, MA*

2*Department of Otology and Laryngology, Harvard Medical School, Massachusetts Eye and Ear Infirmary, Boston, MA*

3*Biopsychology Program, Hunter College, City University of New York, New York*

4*Department of Engineering, Trinity College, Hartford, CT*

Abstract

The occurrence of inappropriate co-contraction of facially innervated muscles in humans (synkinesis) is a common sequela of facial nerve injury and recovery. We have developed a system for studying facial nerve function and synkinesis in restrained rats using non-contact opto-electronic techniques that enable simultaneous bilateral monitoring of eyelid and whisker movements. Whisking is monitored in high spatio-temporal resolution using laser micrometers, and eyelid movements are detected using infrared diode and phototransistor pairs that respond to the increased reflection when the eyelids cover the cornea. To validate the system, eight rats were tested with multiple five-minute sessions that included corneal air puffs to elicit blink and scented air flows to elicit robust whisking. Four rats then received unilateral facial nerve section and were tested at weeks 3–6. Whisking and eye blink behavior occurred both spontaneously and under stimulus control, with no detectable difference from published whisking data. Proximal facial nerve section caused an immediate ipsilateral loss of whisking and eye blink response, but some ocular closures emerged due to retractor bulbi muscle function. The independence observed between whisker and eyelid control indicates that this system may provide a powerful tool for identifying abnormal co-activation of facial zones resulting from aberrant axonal regeneration.

Corresponding Author: James T. Heaton, PhD, Center for Laryngeal Surgery & Voice Rehabilitation, Massachusetts General Hospital, One Bowdoin Square, 11th Floor, Boston, MA 02114, 617-726-0211 (voice), 617-726-0222 (fax), james.heaton@mgh.harvard.edu.
List of authors with full addresses:
Jeff M. Kowaleski, B.S., Tessa A. Hadlock, M.D., Department of Otology and Laryngology, Massachusetts Eye and Ear Infirmary, 243 Charles Street, Boston, MA 02114, 617-573-3898
Roberto Bermejo, Ph.D., H. Philip Zeigler, Ph.D., Biopsychology Program, Hunter College of the City University of New York, 695 Park Avenue, New York, NY 10065, 212-772-5363
David J. Ahlgren, Ph.D., Department of Engineering, MCEC, Room 323, Trinity College, Hartford, CT 06106, 860-297-2588

Keywords

barrel cortex; denervation; facial nerve; palsy; paralysis; regeneration; reinnervation; synkinesis; vibrissae; whisking

1. Introduction

The facial nerve provides innervation to superficial muscles of the face, including those surrounding the mouth and eyes. Damage to this nerve arises from a wide variety of traumatic and pathological conditions, including viral facial paralysis, Lyme disease, skull base tumor removal, and head trauma. Recovery from these conditions is often accompanied by instances of aberrant motor axon regeneration, which is manifested as inappropriate co-contraction of muscles supplied by a common nerve in a condition known as synkinesis. In the United States this condition has an incidence of 2/10,000 annually (Peitersen, 2002). Approximately 15% of patients experiencing transient virally-induced facial weakness undergo delayed recovery, showing no evidence of return of movement within 6 weeks of onset. This group almost always develops some degree of synkinesis. The resulting involuntary narrowing of the palpebral fissure (distance between eyelids) during smiling, and the hypertonicity of the midface and neck during routine facial expressions, are both functionally and esthetically disturbing. Simultaneous co-contraction of antagonistic muscles leads to a frozen quality on the affected side of the face, and inhibits patients' ability to express themselves non-verbally, resulting in significant social isolation and psychological distress.

Because facial nerve innervation is similar in humans, rodents, and lagomorphs, rats and rabbits have often been used as model systems for studying human facial nerve function and regeneration (e.g., Angelov et al., 2005; Guntinas-Lichius et al., 2005; Ozcan et al., 1993). Moreover, because eyelid and whisker muscles are experimentally accessible in these animals, their movements could provide useful functional markers of the precision of facial nerve regeneration. Accordingly, rodent whisker movements and lagomorph eyelid movements have each been used in regeneration experiments. However, in humans, misguided regeneration is likely to produce aberrant movement in *both* eyelid and other facial muscles. Comprehensive study of facial nerve conditions such as synkinesis requires simultaneous study of multiple facial zones associated with branches of the facial nerve. Here we describe instrumentation and behavioral methods for simultaneous bilateral measurement and control of eyelid and whisker movements in head-fixed rats undergoing experimentally induced facial nerve manipulation. The system provides high spatiotemporal resolution of bilateral eye blink and whisking behaviors occurring both spontaneously as well as under stimulus control. Validation testing in 8 normal rats followed by unilateral proximal facial nerve transection in 4 of these rats indicated that the normal degree of independence for motor control served by the ocular and maxillary branches of the facial nerve provides a baseline against which the aberrant contraction patterns associated with synkinesis should be readily identifiable.

2. Materials and methods

2.1 Subjects and head fixation

Subjects were 8 female Wistar-Hannover rats, 60–90 days old. For head fixation, rats were fitted with a light-weight titanium head implant that provided a set of four external attachment points for rigid head fixation. The head implant design and surgical implantation procedures are described in detail by Hadlock et al. (2007). The body restraint device (Figure 1) was a half-pipe measuring 89 cm in length and 15 cm in diameter. The pipe had Velcro® straps positioned at the upper and lower limb locations along the rat body length to provide secure body restraint (without constraining respiratory movements), as well as a third strap positioned

above the center of the back which prevented arching of the back. The head was fixed by lowering the external attachment points of the titanium head implant onto four threaded rods, followed by placement of hand-tightened nuts on the rods to firmly hold the implant, and thus the head (Figure 1B).

2.2 Methods for monitoring eyelid and whisker movements

The monitoring system included two pairs of photoelectric sensors (for bilaterally tracking eyelid and whisker movements), three pneumatic mechanisms (for delivery of stimuli intended to elicit such movements) and recording equipment (for sensor and video data). A system overview is provided in Figure 2.

2.2a Whisker tracking apparatus and methods—The hardware and software used for monitoring whisker movements was adapted from that described by Bermejo and colleagues (1998; 2002). Briefly, movement of a single whisker (C-1) on each side of the head, marked to increase its detectability by the monitoring system (Figure 1C), was independently tracked using two sets of commercial laser micrometers (Figure 3 and Figure 4; RX Series, MetraLight, Santa Mateo, CA). Each micrometer scanline was considered parallel to the lateral surface of the face at 17° from the head midline. Based on the typical adult rat intra- C1-origin distance of 15 mm, the right and left scanlines were positioned 11 mm from each respective C1 origin, providing adequate clearance for the eyelid tracking apparatus (see next section).

Each micrometer pair had a laser emitter (780 nm wavelength light curtain) and a detector comprised of a 28 mm linear array of 4000 charge-coupled devices (CCD scanline). The emitter and detector were aligned at a vertical distance of 10 cm (Figure 4), with the light curtain striking the scanline for detection of objects passing between the emitter/detector pair (e.g. “edge detector”). The laser micrometers were capable of high temporal (0.417 ms response time) and very high spatial resolution (7 μm), and were factory-set in firmware to disregard shadows less than 1 mm wide so that light curtain interruptions (shadows) from unmarked whiskers would be ignored, and only the larger shadow from the marked C1 whisker would be detected. This custom firmware configuration is available on request from the manufacturer.

2.2b. Eyelid tracking apparatus and methods—The present system utilized hardware modified from that described by Thompson, Moyer, Akase and Disterhof (1994), which utilizes infrared (IR) sensors to measure light reflectivity from the cornea and eyelids as the eyelids open and close, respectively. Because the cornea is relatively transparent for IR light compared to the skin and fur of the eyelid, IR reflectivity increases as the lids close over the exposed cornea. In our system, an IR sensor positioned approximately 3.5 to 4 mm from the surface of each eye produced a voltage output relating to changes in IR reflectivity across the entire range of rat eyelid positions, although the relative contribution of the upper versus lower lid was not differentiated.

Each sensor surface was oriented 45° from vertical and 30° relative to the sagittal midline of the head (Figure 3 and Figure 4). The housing of the commercial sensor required reduction in length in order to fit in the limited space between the eyes and the laser micrometers’ vertical light curtain lateral to the face surface. The sensor housing was modified by opening the unit and fixing the IR emitting diode and phototransistor in place using epoxy, the wire leads were bent 90° (upwards) and the plastic housing was trimmed to match the length of the internal components. The LED component of the sensor was located medially for both right and left sensors so that each eye was illuminated similarly. The total length from the center of the sensor face to the back of the unit (when rotated 45°) was 5.4 mm, allowing it to avoid obstructing the optical path of the laser micrometers (see Figure 3). The IR sensors were maintained in a

fixed location such that the eyes were positioned 3.5 – 4 mm from the center of the sensor surface when the C1 whisker origins were positioned as described in section 2.2a.

Eyelid movement was measured in both a binary manner to identify the occurrence of blinks (see section 2.3c), and on a continuous scale for measuring peak closure response using the same software as used for whisking analysis. Sensor output was measured peak-to-peak instead of baseline-to-peak to account for the small reduction in reflected IR light caused by eye retraction during blinking (both in intact and nerve-lesioned rats).

2.2 c. Generation of stimuli eliciting whisking and eyeblink movements—

Computer-controlled air valves were used for two purposes: to deliver air puffs directed at the cornea in order to elicit eye blink, and to deliver sustained flows of scented air towards the snout in order to elicit whisking behavior. The timing of stimulus delivery was on a pseudo-random schedule within each 5 minute testing session. Ten-second air-flows were delivered at random time points, twice within the second minute and once in the fifth minute for a total of 3 air flows per testing period. For air puff delivery to the eyes, six 20 ms puffs were delivered at random, three to each eye. The corneal puffs were not delivered within the first minute, or during the scent delivery air flows. There was a minimum of 2 seconds between corneal air puffs. The time points for each air valve activation were shown on the data acquisition screen and saved in the data file (Figure 5). Spontaneous blinks from one or both eyes ranged from 0–23 per five minute run, but, for quantitative analysis, only elicited blinks were measured to ensure that complete closure was attempted for measured blinks and to note the absence of a reflexive blink response in nerve-lesioned rats.

To elicit whisking, scented air was created by passing air through containers holding olfactants (H/5-20, Colbourn Instruments, Allentown PA) and then directed towards the snout. To deliver scented air flows, pressurized air from our facility was filtered (5 μm) and regulated to 0.5 PSI (MC104-D10TF, Camozzi Pneumatics LTD, Nuneaton, UK) before reaching an electronic valve (VJ114, SMC Inc., Indianapolis, IN) controlled by the data acquisition hardware and software (see section 2.2e, below). The air valve output was directed through a nylon tube to a glass pipette with the tip directed at the rat's snout from a distance of 1–2 mm (Figure 4). The 10 s air flows delivered 17–18 ml of air, and were not strong enough to elicit a consistent somatosensory-based response (e.g. rats did not appear to feel the air flow).

In preliminary experiments, to determine which would consistently elicit robust whisking, multiple olfactants were tested, including peanut butter, pomegranate extract, lavender extract, wet rat chow, soiled bedding, chocolate milk, and dilute isopropyl alcohol, along with other olfactants. Only peanut butter and isopropyl alcohol were consistently effective in eliciting whisking, and these two scents were alternated across recording days for routine scented air flow delivery.

To deliver air puffs to the cornea, pressurized air from our facility was filtered (5 μm) and regulated to 38 PSI before reaching an electronic valve with dual output (HX752.2E1.C212, Matrix Valve Industries, West Greenwich, RI). The independent outputs were directed via polyethylene tubes to small aluminum tubes (1.6 mm ID) mounted on the medial edge of the eyelid sensors (Figure 4). Each tube end was approximately 3.5 to 4 mm from the respective eye surface, with the air puff striking the cornea in a medial-to-lateral direction to avoid contralateral eye stimulation. The valves had an opening response time of < 7 ms, ejecting 2 ml of air at each 20 ms valve activation (puff), which reached the cornea with a latency of 18 ms from the computer's indication of valve activation. These supply pressure and puff duration values were determined in preliminary experiments by making adjustments until rats consistently produced an ipsilateral blink, but only occasionally produced a bilateral blink response (see Results section).

2.2d Data acquisition hardware and analysis software—The data acquisition system included a standard PC with a digital I/O card (KPCI-PIO96, Keithley Instruments Inc., Cleveland, Ohio) to receive the digital output of right and left whisker-tracking laser micrometers, and an A/D card (KPCI-3110) to receive the right and left photoelectric eyelid signals along with the single load cell tracking mandible movement (see system outline in Figure 2). These inputs to the A/D card were sampled at 1 kHz with 12 bits of resolution. Output from the A/D card provided a timing signal to the I/O card for acquisition of the laser micrometer signal at a sampling rate of 1 kHz through an interface board (PB-24SM, Keithley Instruments Inc.). The interface board also contained four solid state I/O modules (SM-ODC5) for controlling the right and left corneal air puff valves and two different scented air flow valves. The interface board could hold up to 24 I/O modules for the addition of other operant learning components (sounds, lights, food delivery, etc.).

A low-force sensing load cell (FS20, 0–750 g; Measurement Specialties Inc., Hampton, VA) was positioned under the mandible to detect potential movements of the restrained head and jaw. It contacted the mandible using a plastic extension from the cell's platform (Figure 4). The cell was slightly pre-loaded against the mandible using mounting hardware with adjustable elevation. In order to compensate for the pre-loaded output voltage and achieve maximum sensitive across a narrow range of applied force, the load cell was attached to a custom circuit that enabled DC-offset and gain control for the cell's 0–5V output using a standard dual-channel operational amplifier (LM6132, National Instruments).

The IR photoelectric apparatus monitoring eyelid movement was based on a Fairchild Semiconductor reflective object sensor, type QRB1114, which consists of an infrared emitter and a phototransistor. The device provided non-contact sensing of eye blink, convenient transistor output, and easy adjustment of sensor position. The sensor had optimal sensitivity at a distance of 4 mm from the eye with a coverage spot about 5 mm in diameter (see www.fairchildsemi.com/ds/QR/QRB1114.pdf). In our system, the QRB1114 emitted an IR beam modulated at 5.2 kHz. As Figure 6 shows, the reflected signal was amplified and sent through a four-pole bandpass filter that rejected signals from low-frequency ambient light sources. The detector and output amplifier scaled the output voltage to the range 0 – 5 V.

The IR photoelectric sensor circuit was built on a custom four-layer board. The sensitivity and frequency response of this system was tested by placing the sensor 2–6 mm in front of an IR reflective surface that was stuck by a piston driven by a voice coil (TruTone Electrolarynx, Griffin Laboratories, Temecula, CA) at 40 – 200 Hz. An accelerometer (BU7135, Knowles Electronics, Inc., Itasca, IL) was attached to the reflective surface to monitor displacement (vibrations) caused by the piston. The IR sensor system output was sensitive to both the distance that the surface was held relative to the IR sensor (DC component), and to the brief surface displacements caused by the piston, demonstrating an ability to capture the full potential range of frequency components for eyelid movement.

A digital video camera (Optura Pi, Canon, Inc., Lake Success, NY) was mounted facing the front of the tested rat, enabling the equipment operator to unobtrusively monitor behavior during recording sessions. This video signal was split-screen mixed with an s-video output from the data acquisition computer's video card (WJ-MX20, Yamaha Inc. Buena Park, CA), providing a real-time representation of the ongoing signal acquisition along with a view of the rat face. The mixed video was recorded by a second digital video camera and stored for future reference.

2.3 Behavioral and surgical procedures

2.3a Adaptation to head fixation and body restraint—To reduce stress during their subsequent restraint in the testing apparatus, animals were handled daily for 2 weeks prior to

surgery for placement of the head mount. One week after this surgery rats were placed in the body restraint apparatus daily for a week, with head restraint added to the daily conditioning the following week. By the third week after head mount implantation surgery, rats were typically sufficiently conditioned to undergo head/body restraint without struggling or signs of stress, and were therefore ready to begin participating in data collection. Rats were not food or water deprived prior to testing.

For restraint, rats were first placed in a bag covering the body and limbs. Bags used for this purpose were disposable plastic cone-shaped bags (DeCapicone®; Braintree Scientific, Braintree, MA) with an opening cut out for the head, or washable fabric bags (Figure 1) with openings at both ends and draw strings that could be cinched using plastic cord stops (barrel toggles). The bagged rat was then placed in the body restraint device and its head fixed, as described above (section 2.1).

Initially, C-1 whiskers were marked bilaterally using a rectangular strip of lightweight adhesive foam (Bermejo et al., 1998), but this occasionally adhered to adjacent whiskers and disrupted the movement signal. Following Dr. Cornelius Schwarz (personal communication, 2006), we now use a pair of thin, rigid and lightweight polyimide tubes (SWPT-045, SWPT-008, Small Parts Inc.; see Figure 1). One tube 19 mm in length with an internal diameter approximately the size of the whisker's outer diameter (near the whisker pad; ID 0.226 mm) is glued inside a larger tube (length = 15 mm, ID 1.15 mm) that interrupts the micrometer light curtain much more than adjacent unmarked whiskers. This makes the marked C1 whiskers selectively visible to the laser micrometers (see section 2.2a), allowing it to be tracked in the presence of neighboring whiskers. Each tube pair weighs 3–4 mg, and markers of this size and approximate weight have been shown by Bermejo et al (1998) not to alter whisking function. The tubes are easily threaded onto the C1 whisker after applying a small amount of water-soluble lubricant, and are gently removed at the end of each test session.

After application of the markers, the restraint hardware was placed onto an adjustable stage for positioning of the rat relative to the whisker and eyelid sensors of the recording system (see below). Rats were typically tested within 5 minutes of being placed in restraint, and released immediately thereafter, for a typical restraint time of 15 minutes or less. Having multiple sets of restraint equipment allowed us to prepare rats while the recording system was in use with another animal. Therefore, two investigators working together (one performing the recording with the other restraining/releasing rats) could easily record 30 or more rats a day using only one recording system.

2.3b. Positioning the restrained rat with respect to the sensors—Accurate measure of eyelid and whisker movement depends on precise placement of the monitored anatomy relative to the sensors. Software calculation of horizontal whisker movement angle and velocity was performed by tracking the instantaneous C1 whisker location along the photoelectric scanline of commercial laser micrometers (described above) in relation to the C1 origin. We designated the midpoint of the right and left scanlines as the whisker 0° location, and used a pair of class IIIa lasers to cast a visible beam that identified the desired C1 origin locations (Figure 4). A third laser cast a curtain of light along the apparatus midline, falling along the rat head sagittal plane when the rat was positioned correctly relative to the right and left micrometers. For most rats, when the lasers simultaneously illuminated the C1 origins and head midline, the eyes were also appropriately aligned with the two IR eyeblink sensors. A pair of IR-sensitive cameras (Lorex SG6153), located 8 cm lateral and slightly posterior/inferior to the eyes, showed the illumination pattern on the face from the IR light emitted from the right and left sensors, and adjustments in rat head rotation were made if the eyes were not evenly illuminated (see section 2.2c below). Small changes in the C1 origin height due to head roll (relative to the long axis of the body), when required to achieve symmetrical eye

illumination, did not influence whisker tracking, since each micrometer emitter/detector pair could accurately sense the intervening tagged whisker at any potential C1 origin height.

An adjustable platform held the rat restraint apparatus and allowed manipulation of rat orientation in multiple dimensions to achieve the desired head positioning. The platform featured two U-shaped sections, with an ID that matched the OD of the rat restraint half-pipe. These supports were positioned 15 cm apart to contact both the front and back of the restraint half-pipe, and allowed the unit to roll on its long axis in reference to ruled markings. The platform holding the restraint apparatus (CR Scientific Laboratory Scissor Jack) was height-adjustable, and contained a large-format microscope stage (Carl Ziess, Oberkochen, Germany), thereby providing X-Y-Z position control of the platform surface. Moreover, the platform's uppermost horizontal surface could rotate around a midline point centered under the rat's head to allow yaw control relative to a scale in degrees located on the opposite end of the horizontal platform. Since the head restraint implants were consistently secured parallel to the dorsal surface of the calvarium with little variation in vertical height along the rostrocaudal axis, pitch control for the head was not needed.

2.3c. Measurement of Correspondence between Whisking and Blinking Behavior—To explore the potential utility of the apparatus to examine the independence (or interdependence) of whisking and eye blink function, we examined whether animals moved their eyelids during elicited whisking, and how often induced blinking occurred coincidentally with whisking. For each testing run, the areas of stimulation, (either scented air flow or corneal air puff), were examined for whether they elicited whisking and/or blinking. The following dichotomous events were recorded: right whisk with olfactory stimulus, left whisk with olfactory stimulus, right blink with olfactory stimulus, left blink with olfactory stimulus, right puff-induced ipsilateral blink, right puff-induced ipsilateral whisk, right puff-induced contralateral blink, right puff-induced contralateral whisk, and similar parameters for the left side. The criteria utilized for this binary yes/no analysis included the following: Any onset of three or more contiguous whisks averaging $\geq 12°$ in magnitude, or change in average ongoing whisking by $\geq 12°$ during the 10 s scented air flow was considered elicited whisking. Any onset or change of one or more whisks by $\geq 12°$ within 100 ms of the corneal air puff was considered elicited whisking. Any eyelid signal of at least 100 mV (approximately 10% of the range of the maximum eye signal response) with ≥ 5 ms/ms slope occurring during the 10 s scented air flow or initiated within 100 ms of the corneal air puff was considered an elicited blink.

2.3d. Sham and Facial Nerve Surgery—All animals underwent a sham surgical procedure whereby the left facial nerve was exposed. General anesthesia was induced via an intramuscular injection of ketamine (50 mg/kg) and medetomidine (0.5 mg/kg) mixed in saline. Left facial nerve exposure involved a pre-auricular incision, reflection of the parotid gland, and visual identification of the main trunk of the facial nerve. The parotid was then laid back into appropriate position, and the wound closed in a single layer. Rats were allowed to recover on a warming pad, and were monitored for food and water intake, post-operative discomfort, and weight gain. On postoperative days 10 and 20 eyelid and whisker movements were monitored as described above with five-minute recording sessions.

Subsequently, four of the eight animals underwent complete left facial nerve transection. Anesthesia induction and surgical dissection were performed as described above, and a 1 cm segment of the facial nerve trunk was excised. The proximal stump near the stylomastoid foramen was buried into adjacent neck musculature to discourage face muscle reinnervation. Weekly post-operative testing of the animals began three weeks after nerve section for the ensuing 3 weeks.

3. Results

There were no problems with head restraint implant extrusion or infection over the study period. Animals exhibited normal cage behavior, and gained or maintained weight appropriately. On approximately 20% of the recording sessions animals would struggle in the head fixation apparatus or maintain a stressed facial posture (e.g. eyes held closed) during data collection, necessitating repetition of the five-minute testing session after further adaptation, with the last recording then used for data analysis.

3.1. Bilateral whisker movement

All animals exhibited symmetric whisking after surgical exposure of the left facial nerve, with average whisking amplitudes of 32.8° and 32.5° degrees on the right and left sides, respectively. These values match closely those previously reported (32.8, SE 0.96, Bermejo et al., 1998) using the same type of CCD array for whisking detection, as do values for average whisking velocity and acceleration (see Figure 7). Complete left facial nerve transection (n=4) initially abolished ipsilateral whisker movements, and resulted in a complete absence of ipsilateral whisking of at least 15° for any animal until week 6 after nerve lesion, at which point one rat had partial recovery of whisking (Figure 7).

3.2. Bilateral eyelid movement

Assessment of eye blink occurrence revealed that non-lesioned animals responded to an air puff with an ipsilateral eye closure 100% of the time (see Table 1). Eyelid peak amplitude for puff-induced blinks was similar for right and left eyes prior to nerve section, but was relatively low ipsilateral to facial nerve section throughout the 6 weeks of post-surgical testing (Figure 8). Although rats appeared unable to close their affected eye upon recovery from surgical anesthesia, they all acquired the ability within the first postsurgical week, and showed no clinically significant corneal exposure. Although rats were able to blink after facial nerve lesion, their eyelid closure in response to corneal air puff had clearly changed. Eyelid closure was typically complete in response to corneal air puff, but was often only partial in the eye ipsilateral to facial nerve lesion.

3.3. Comparison of whisker and eyelid movement

The occurrence of whisking and blinking associated with corneal air puff and scented air flow is presented in Table 1. Before nerve injury, we observed that the scented air flow led to whisking behavior on 79.2% of the flow presentations, and led to eye blink in 8.3% of the presentations. Corneal air puff delivery resulted in an ipsilateral blink 100% of the time, and contralateral eye blink 8.3% of the time. Corneal air puffs induced and/or affected ipsilateral whisking behavior an average of 41.7% of the time, and contralateral whisking an average of 29.2% of the time before lesion. Overall, blinking and whisking were largely independent, with 58 – 92% separation in blinking and whisking elicited by corneal air puff and scented air flow, respectively.

Following unilateral facial nerve transection, scented air flow and corneal air puffs failed to elicit whisking on the denervated (left) side of the face in all animals throughout the six weeks of postoperative testing (see Table 1). Blinking response from the left eye was often present but consistently reduced relative to the right eye during both corneal air puffs and scented air flows. Whisking and eyelid movement on the intact (right) side of the face persisted after contralateral facial nerve lesion. The persistence of right-sided puff-induced whisking and blinking to left corneal puffs indicate that the left cornea was still sensitive despite reduced blink behavior after ipsilateral facial nerve lesion.

4. Discussion

In this report we have described the procedures and apparatus for assessing facial nerve function in restrained rats. Specifically, the methods provided here enable simultaneous bilateral monitoring of eyelid and whisker movements, achieving a critical, comprehensive assessment of facial nerve function not previously attainable through the study of eyelid and whisker movements in isolation. The *in vivo* data presented demonstrate the utility of this system in characterizing the independence of facial zones supplied by particular branches of the facial nerve. The ability to perform repeated, non-contact testing offers data regarding the time frame of recovery of distinct facial functions, and permits comparison of ocular versus midfacial recovery. Perhaps most importantly, we have brought eyelid and whisker movement under stimulus control, demonstrating that these behaviors are normally largely independent of each other. By analyzing the response of one facial zone while another zone is stimulated, our system potentially provides an opportunity to measure the phenomenon of synkinesis in the rat when multiple facial motor functions become coupled due to aberrant reinnervation.

Because synkinesis is the single most common complaint among patients suffering from delayed recovery after Bell's Palsy, Ramsay Hunt syndrome, Lyme-associated facial paralysis, and other clinical neuritides, a laboratory model for its quantification is long overdue. Synkinesis is also an inevitable sequela of nerve regeneration across a neurorrhaphy or through a nerve graft after proximal nerve lesion where functionally diverse axons travel together. The apparatus and animal model described here will permit the characterization of the independence (or interdependence) of rodent ocular and vibrissial facial function in normal animals, as well as in lesioned or diseased states as we have preliminarily shown. Thereafter, investigators interested in treating synkinesis can utilize this quantitative functional testing apparatus to assess the effect of different pharmacologic, tissue engineering, or surgical interventions on synkinesis mitigation. Effective treatment regiments may be directly applicable to synkinesis observed in other motor systems, such as laryngeal control (Crumley, 2000, 1979), where debilitating synkinesis commonly results from nerve supply lesion or disease.

In addition to studying facial lower motor neuron function, the present system allows study of interactions between the whisker and eyeblink CNS systems. This capability is of interest in the light of recent studies which have shown that mystacial vibrissae stimulation may be used as a conditioned stimulus (CS) for trace eyeblink conditioning (Das et al., 2001; Galvez et al., 2006; Troncoso et al., 2004), and that cortical barrel lesions impair such trace associations (Galvez et al., 2007). Many of these studies detect eyelid or nictitating membrane movement using IR reflectance methods similar to those used in the present report (Das et al., 2001; Galvez et al., 2007; Galvez et al., 2006), but they do not provide an integrated means of simultaneously tracking whisking. The simultaneous, bilateral measurement of whisking and eyelid movement will be crucial for describing the brain mechanisms mediating coordination in the control of these behaviors.

Although our system utilizes a common method for non-invasively measuring eyelid movements via reflective object sensors (Ryan et al., 2006; Thompson et al., 1994), one disadvantage of opto-electronic eyelid movement sensors is that they do not easily differentiate active eyelid movement resulting from contraction of the orbicularis oculi versus passive eyelid movement resulting from eye retraction into the orbit. After unilateral facial nerve section, rats were observed during handling to achieve complete bilateral eyelid closure within the first post-operative week (before regeneration of the cut facial nerve could possibly occur), demonstrating a substantial degree of residual or compensatory eyelid movement independent of facial nerve function. Moreover, the corneal surface of the eye ipsilateral to facial nerve lesion did not show signs of chronic irritation or dehydration (e.g. no discoloration, ulceration, etc.), suggesting that rats were able to blink with sufficient frequency to maintain a tear film

and avoid the potential sequelae of eyelid paralysis. Nevertheless, eyelid movement ipsilateral to facial nerve lesion was clearly affected, as shown by the reduced average eyelid sensor amplitude in response to corneal air puff and reduced occurrence of blinking in response to corneal air puffs and scented air flows.

Immediately after facial nerve lesion, the retractor bulbi musculature has been shown to support blink response in rabbits (Leal-Campanario et al., 2004), and can do the same in cats after several weeks as they progressively increase activity of the eye retractor bulbi motor system to compensate for lost orbicularis oculi function (Delgado-Garcia et al., 1990; Gruart et al., 2003). These extraocular muscles are not innervated by the facial nerve, but rather by axons originating in the accessory abducens nucleus (Crandall et al., 1981; Delgado-Garcia et al., 1990; Oda, 1981), and are thus spared during facial nerve lesion. Similar retractor bulbi muscles have been described in rats (Khanna and Porter, 2001; Oda, 1981), although their role in supporting blinking behavior has not been described. Direct measurement of orbicularis oculi electromyography in conjunction with search coil tracking in a magnetic field has been used in prior studies (Gruart et al., 1995; Gruart et al., 2003; Koekkoek et al., 2002) as an indicator of eyelid motor activation and lid movements (respectively), but have the disadvantage of potential morbidity from hardware implantation and chronic maintenance in soft tissues, and challenges in relating EMG signals with palpebral fissure (upper and lower eyelid position). We are currently studying the relative contribution of retractor bulbi and orbicularis oculi musculature in rat blink function through combinations of denervation and myotomy using the present opto-electronic eyelid movement sensors with the goal of identifying eyelid response features (e.g. signal magnitude, latency, slope, etc.) that distinguish among these muscle groups.

5. Conclusions

Measured whisking and eyeblink behavior using our system occurred both spontaneously and under stimulus control, with no detectable difference from previously published normative data of horizontal whisking. Proximal facial nerve section caused an immediate ipsilateral loss of whisking and eyelid movement, with some eyelid movement emerging early in the first post-surgical month, suggesting a compensatory function by the retractor bulbi muscles. The normal and experimentally-induced independence observed between whisker and eyelid control suggests that studies of facial nerve regeneration and cortical function using this system should be able to detect abnormal co-activation of facial zones (synkinetic facial movement) associated with aberrant axonal regeneration. Finally, although our focus here is on methods for the study of aberrant co-activation of whisker and eyeblink systems, our methodology will also facilitate study of normal interactions between these two systems by providing simultaneous, bilateral measurement of whisking and eyelid movement needed for studying the central associative mechanisms coordinating these behaviors.

6. Acknowledgments

This work was supported by grants K-08 DE015665-01A2 to T.A.H. and NS048937 to H.P.Z. We thank Christopher Scarpino for his engineering assistance in hardware design and fabrication.

7. References

Angelov DN, Guntinas-Lichius O, Wewetzer K, Neiss WF, Streppel M. Axonal branching and recovery of coordinated muscle activity after transection of the facial nerve in adult rats. Adv Anat Embryol Cell Biol 2005;180:1–130. [PubMed: 16261803]

Bermejo R, Houben D, Zeigler HP. Optoelectronic monitoring of individual whisker movements in rats. J Neurosci Methods 1998;83:89–96. [PubMed: 9765121]

Bermejo R, Vyas A, Zeigler HP. Topography of rodent whisking--I. Two-dimensional monitoring of whisker movements. Somatosens Mot Res 2002;19:341–346. [PubMed: 12590835]

Crandall WF, Goldberg SJ, Wilson JS, McClung JR. Muscle units divided among retractor bulbi muscle slips and between the lateral rectus and retractor bulbi muscles in cat. Exp Neurol 1981;71:251–260. [PubMed: 7449900]

Crumley RL. Laryngeal synkinesis revisited. Ann Otol Rhinol Laryngol 2000;109:365–371. [PubMed: 10778890]

Crumley RL. Mechanisms of synkinesis. Laryngoscope 1979;89:1847–1854. [PubMed: 502707]

Das S, Weiss C, Disterhoft JF. Eyeblink conditioning in the rabbit (Oryctolagus cuniculus) with stimulation of the mystacial vibrissae as a conditioned stimulus. Behav Neurosci 2001;115:731–736. [PubMed: 11439462]

Delgado-Garcia JM, Evinger C, Escudero M, Baker R. Behavior of accessory abducens and abducens motoneurons during eye retraction and rotation in the alert cat. J Neurophysiol 1990;64:413–422. [PubMed: 2213125]

Galvez R, Weible AP, Disterhoft JF. Cortical barrel lesions impair whisker-CS trace eyeblink conditioning. Learn Mem 2007;14:94–100. [PubMed: 17272654]

Galvez R, Weiss C, Weible AP, Disterhoft JF. Vibrissa-signaled eyeblink conditioning induces somatosensory cortical plasticity. J Neurosci 2006;26:6062–6068. [PubMed: 16738249]

Gruart A, Blazquez P, Delgado-Garcia JM. Kinematics of spontaneous, reflex, and conditioned eyelid movements in the alert cat. J Neurophysiol 1995;74:226–248. [PubMed: 7472326]

Gruart A, Streppel M, Guntinas-Lichius O, Angelov DN, Neiss WF, Delgado-Garcia JM. Motoneuron adaptability to new motor tasks following two types of facial-facial anastomosis in cats. Brain 2003;126:115–133. [PubMed: 12477700]

Guntinas-Lichius O, Irintchev A, Streppel M, Lenzen M, Grosheva M, Wewetzer K, Neiss WF, Angelov DN. Factors limiting motor recovery after facial nerve transection in the rat: combined structural and functional analyses. Eur J Neurosci 2005;21:391–402. [PubMed: 15673438]

Hadlock T, Kowaleski J, Mackinnon S, Heaton JT. A novel method of head fixation for the study of rodent facial function. Exp Neurol 2007;205:279–282. [PubMed: 17397835]

Khanna S, Porter JD. Evidence for rectus extraocular muscle pulleys in rodents. Invest Ophthalmol Vis Sci 2001;42:1986–1992. [PubMed: 11481262]

Koekkoek SK, Den Ouden WL, Perry G, Highstein SM, De Zeeuw CI. Monitoring kinetic and frequency-domain properties of eyelid responses in mice with magnetic distance measurement technique. J Neurophysiol 2002;88:2124–2133. [PubMed: 12364534]

Leal-Campanario R, Barradas-Bribiescas JA, Delgado-Garcia JM, Gruart A. Relative contributions of eyelid and eye-retraction motor systems to reflex and classically conditioned blink responses in the rabbit. J Appl Physiol 2004;96:1541–1554. [PubMed: 14578372]

Oda Y. Extraocular muscles and their relationship to the accessory abducens nucleus in rats as studied by the horseradish peroxidase method. Okajimas Folia Anat Jpn 1981;58:43–54. [PubMed: 7279383]

Ozcan G, Shenaq S, Spira M. Vascularized nerve tube: an experimental alternative for vascularized nerve grafts over short gaps. J Reconstr Microsurg 1993;9(9):405–413. [PubMed: 8283420]

Peitersen E. Bell's palsy: the spontaneous course of 2,500 peripheral facial nerve palsies of different etiologies. Acta Otolaryngol Suppl 2002:4–30. [PubMed: 12482166]

Ryan SB, Detweiler KL, Holland KH, Hord MA, Bracha V. A long-range, wide field-of-view infrared eyeblink detector. J Neurosci Methods 2006;152:74–82. [PubMed: 16257057]

Thompson LT, Moyer JR Jr, Akase E, Disterhoft JF. A system for quantitative analysis of associative learning. Part 1. Hardware interfaces with cross-species applications. J Neurosci Methods 1994;54:109–117. [PubMed: 7815815]

Troncoso J, Munera A, Delgado-Garcia JM. Classical conditioning of eyelid and mystacial vibrissae responses in conscious mice. Learn Mem 2004;11:724–726. [PubMed: 15537734]

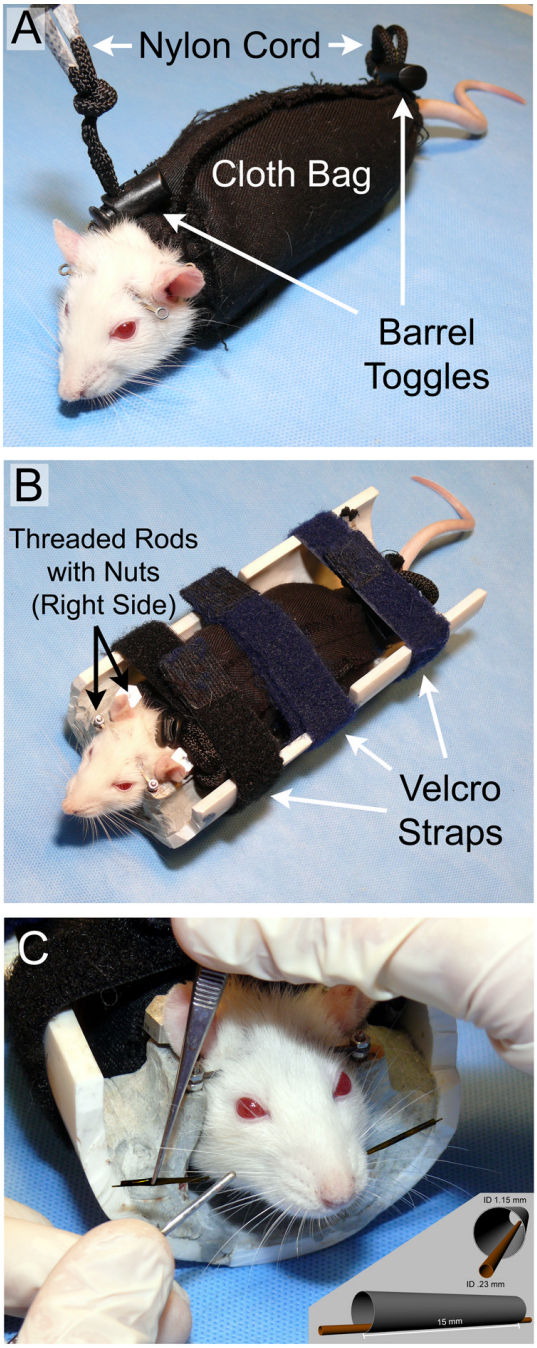

1.

A) Rat in soft restraint consisting of a washable cloth bag with nylon cords and toggle barrels constricting the two ends of the bag. B) Rat in rigid restraint apparatus containing an interface for the titanium head implant to mate with the polymer half-pipe over threaded rods and nuts, as well as the three Velcro strap locations at the limbs and across the mid back. C) Application of polyimide tubes used to enhance the detectability of the C1 whiskers. The outer tube is grasped with forceps as the inner tube is threaded onto the C1 whisker. The insert shows enlarged schematic views of the marking tube eccentric configuration.

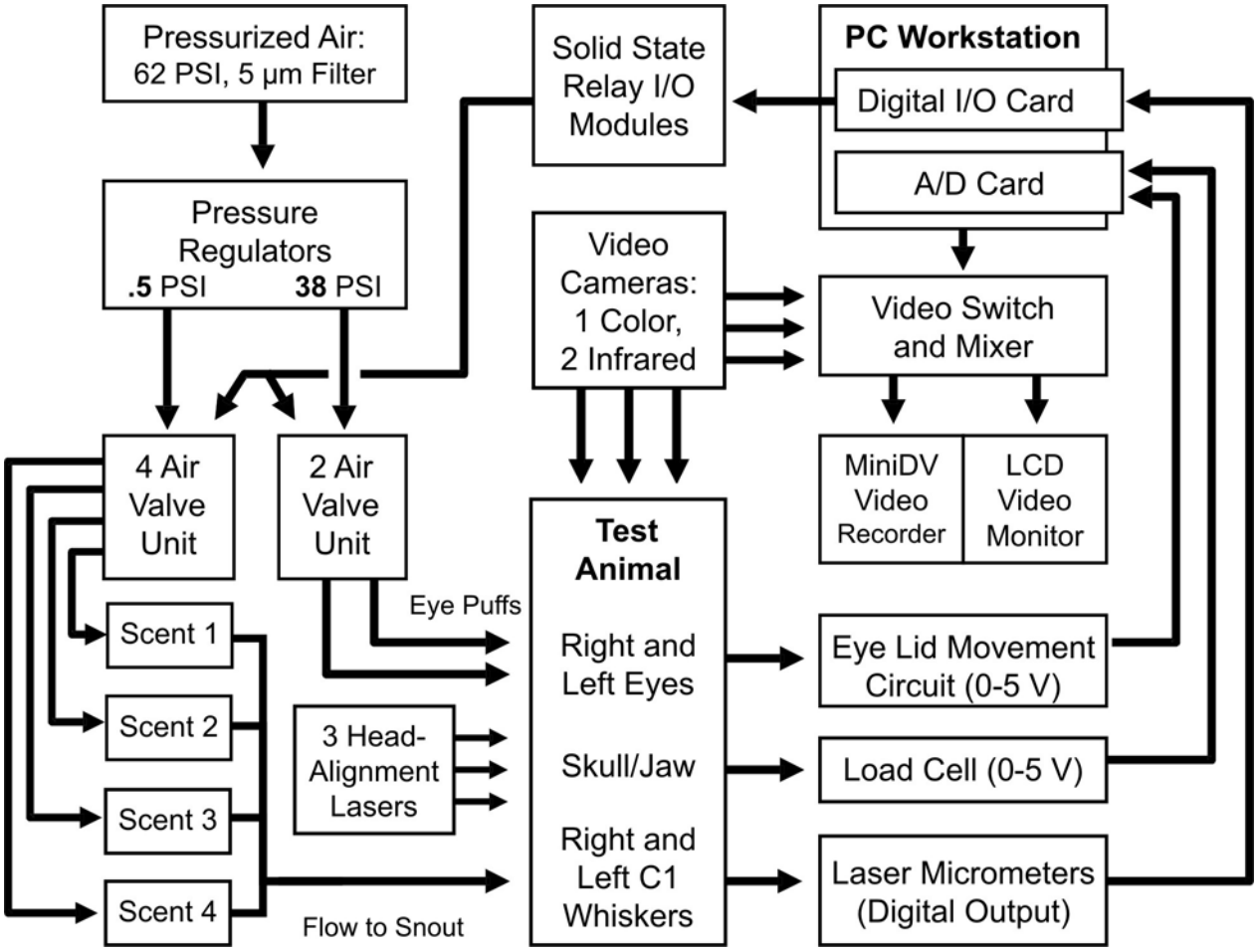

2.

Recording system overview, showing the major data acquisition and behavioral control components.

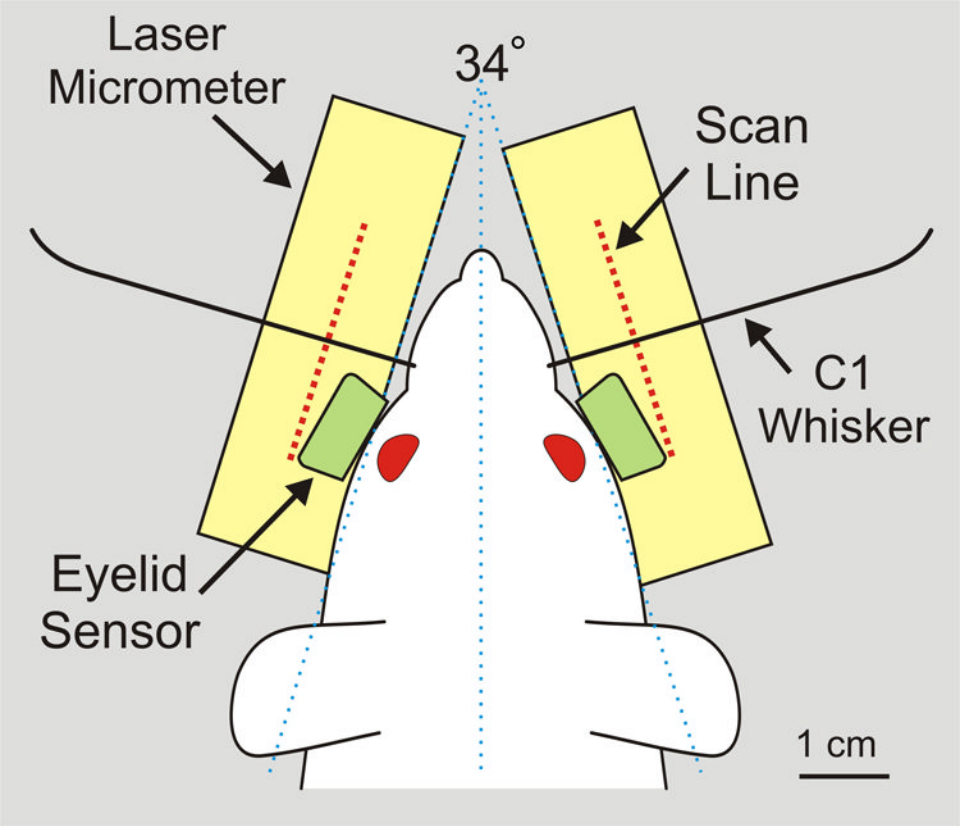

3.

Overhead view of rat with C1 whisker origins centered on the laser micrometer scanlines at a distance of 11 mm. Eyelid sensors are positioned 3.5 – 4 mm in front of each cornea, yet do not obstruct the optical pathway between laser emitter and scan line of the micrometer pairs.

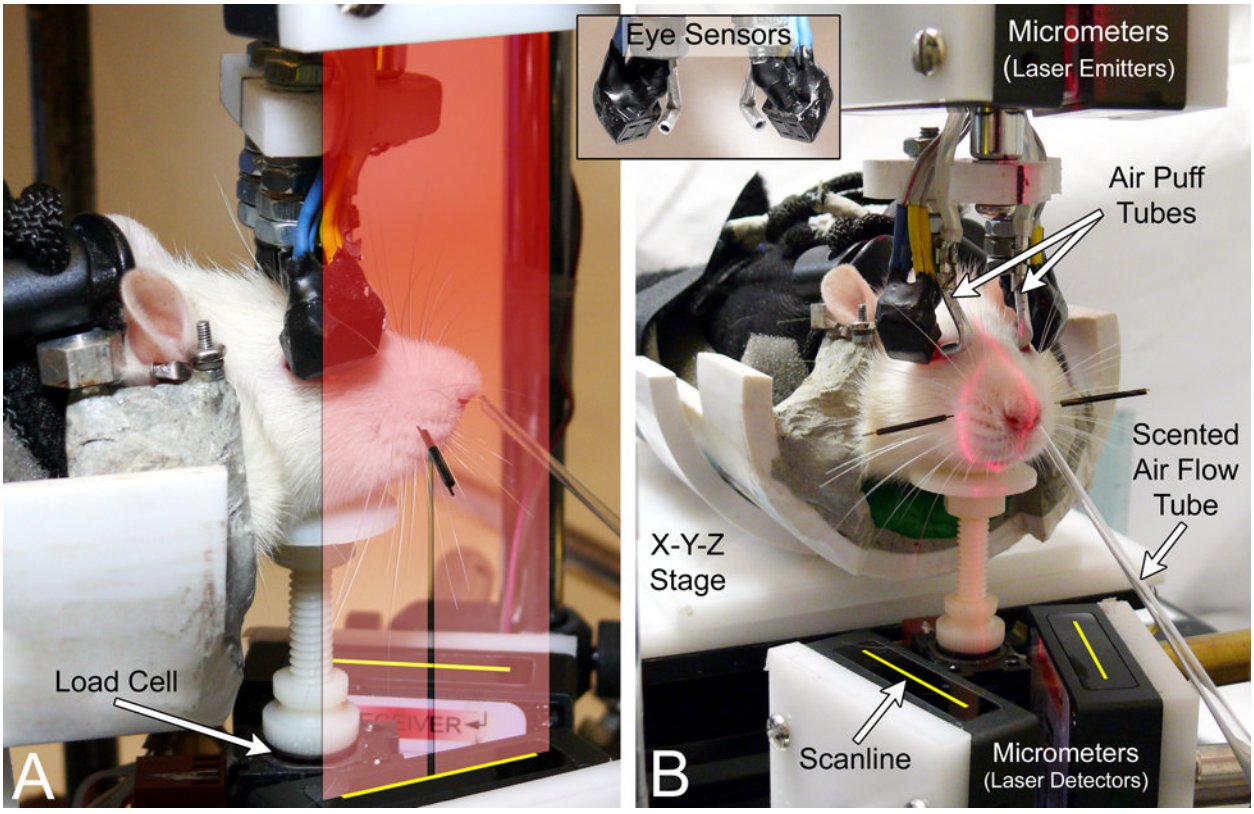

4.

Photographs of a rat in position for testing facial nerve function. A) View of the right face showing a graphic representation of the laser light curtain cast from the right micrometer emitter 10 cm above the detector, and the shadow cast by the lightweight tube on the right C1 whisker. The micrometer detector scanlines are graphically depicted as yellow lines (added to the photos) and can track the C1 whisker movement by detecting where the light curtain is interrupted. B) Anterior view of the face, showing the tubes that deliver right/left corneal air puffs and the scented air flow. The insert (between A and B) shows the infrared eye sensor emitter/detector surface and corneal air puff tube openings. The red laser light visible on the snout indicates the sagittal plane and intersection of the C1 whisker relative to the center of the ipsilateral scanline. These registration lasers are used to position the rat relative to the stationary sensors using the X-Y-Z adjustable stage and restraint rotation capabilities, and are extinguished prior to data recording.

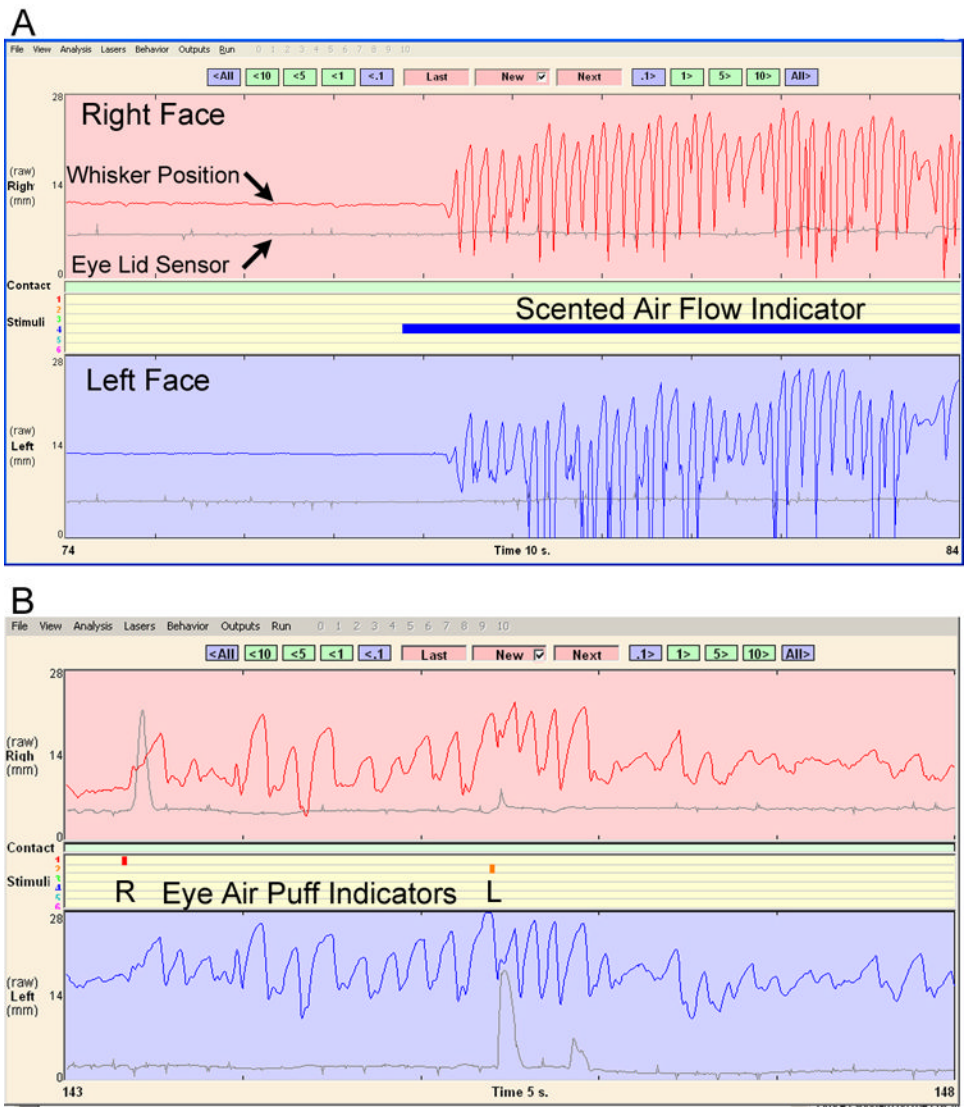

5.

Whisking and eyelid movement data examples from the acquisition and analysis software's data review screen. A) Ten seconds of data are shown, with brisk whisking elicited by the presentation of a scented air flow (solid blue bar). The top half (pink background) presents the whisker position (in red) and eye sensor signal (in gray) for the right face, whereas the bottom half (pale blue background) presents the whisker position (in blue) and eye sensor signal (in gray) for the left face. B). Five seconds of data are shown, with eye blinks elicited by right and left air puffs (see small red and orange markers in the center, respectively). Note how each air puff caused an ipsilateral eye blink, and that bilateral whisking began with the first corneal air puff and continued through the second air puff with only slight alteration.

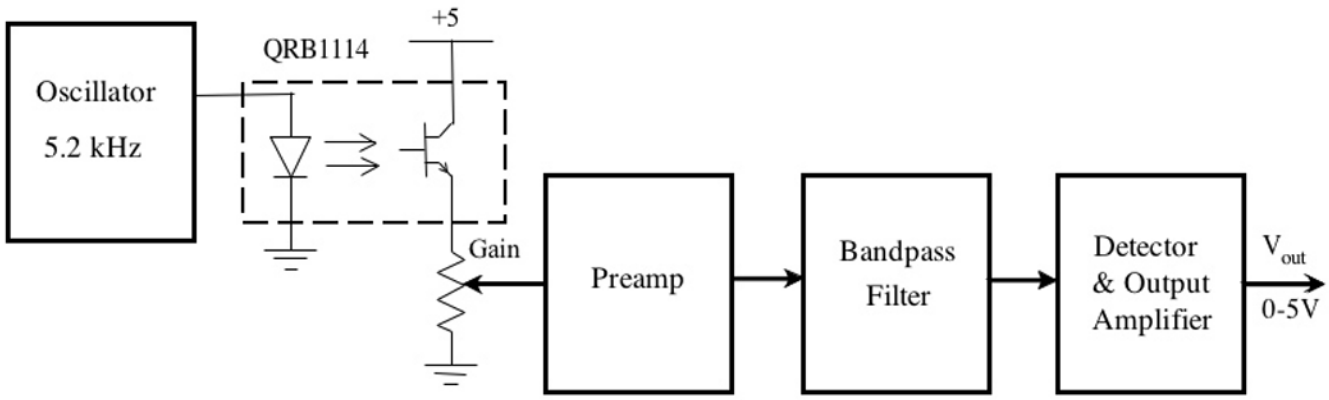

6.

Block diagram of the eyelid movement detection circuit. The infrared sensor (QRB1114) is surrounded by dotted lines, and was the component positioned approximately 4 mm in front of the eye to detect changes in light reflectivity as the eyelids closed and opened. There was an independent sensor and signal output for each eye, although only a single channel is depicted in the diagram.

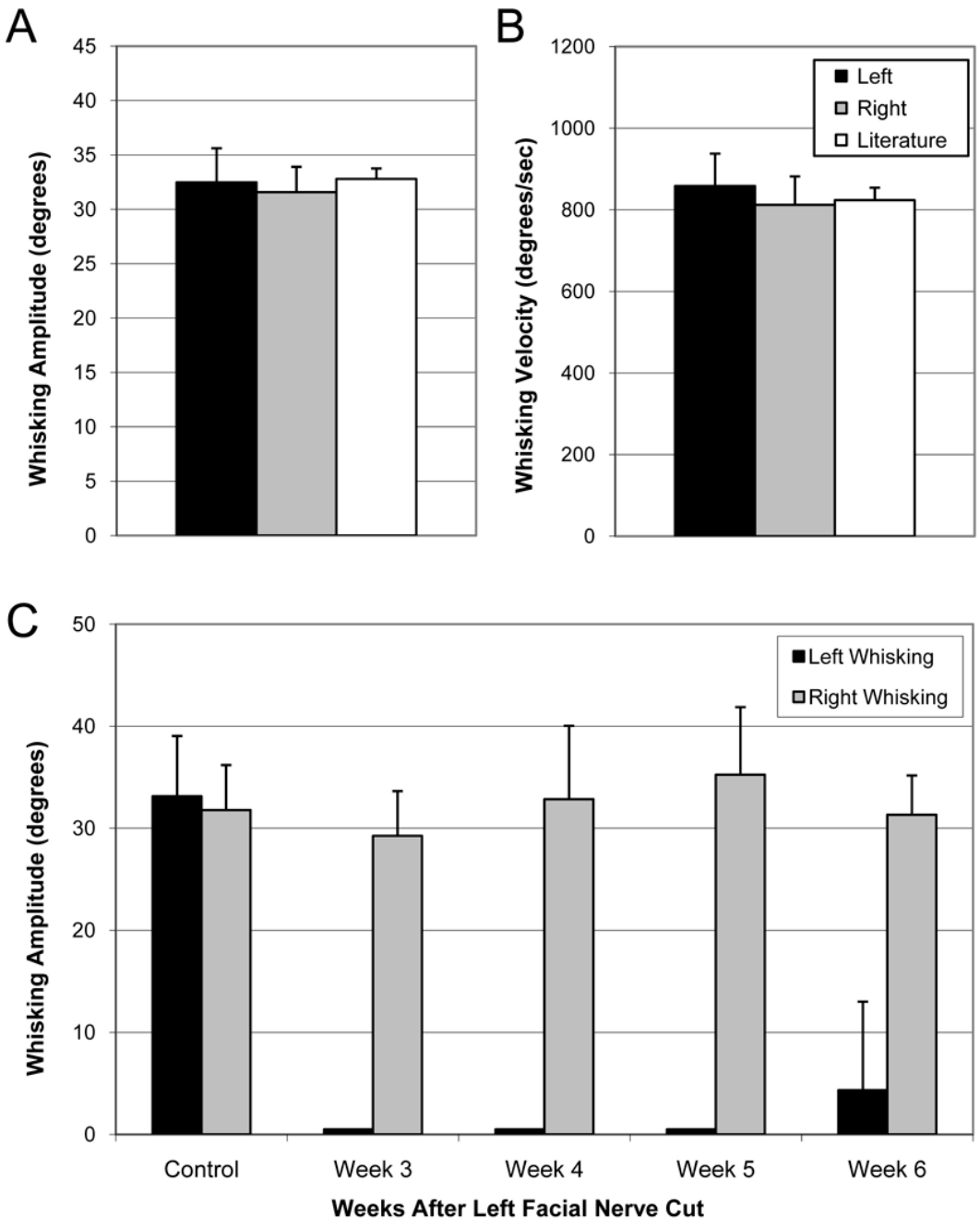

7.

Pre-lesion whisking amplitude (A) and velocity (B) are shown for 8 normal rats compared to bilateral values reported by Bermejo et al., 1998. Whisking amplitude is also shown for pre versus post left facial nerve lesion (C; N = 4), with a complete absence of left whisking on weeks 3–5, and one animal demonstrating partial recovery of left side whisking by week 6 (error bars are +S.E. in A and B, and +S.D. in C).

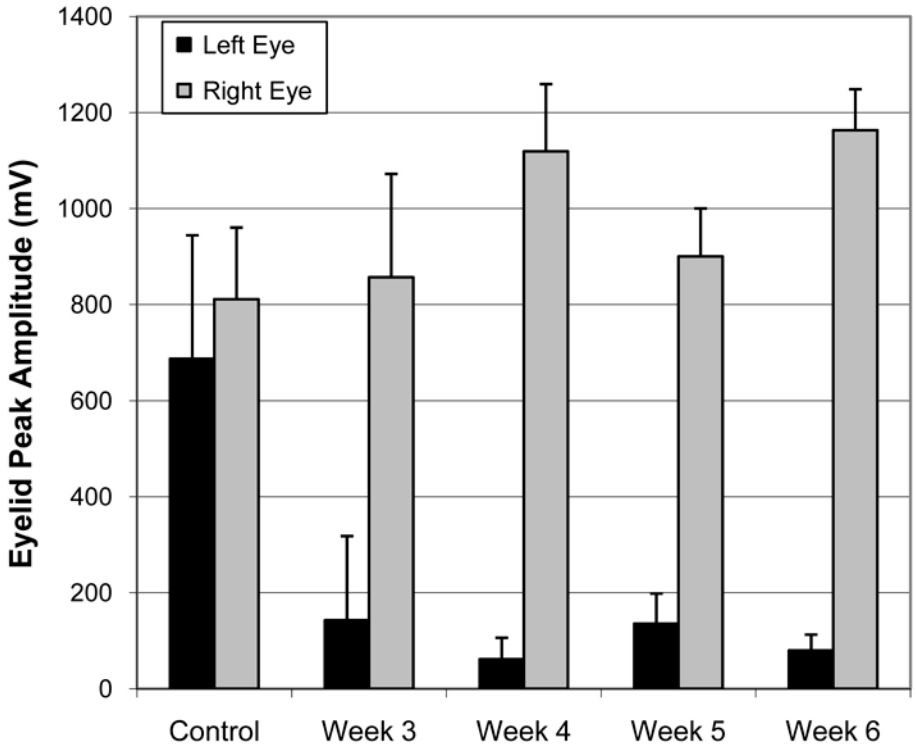

8.

Eyelid peak amplitude for pre versus post left facial nerve lesion (N = 4), with a reduction in left eyelid amplitude that persisted across post-surgical weeks 3–6 (error bars are + S.D.).

Table 1

Average percent occurrence for whisking and blinking behavior during scented air flows and corneal air puffs before versus weeks 3–6 after left nerve lesion (N = 4). Function is indicated separately in each cell for the left (L) and right (R) side of the face.

	Scent-induced whisks		Scent-induced blink		Ipsilateral puff-induced blink		Contralateral puff-induced blink		Ipsilateral puff-induced whisk		Contralateral puff-induced whisk	
Before Nerve Lesion	L	79.2	L	8.3	L	100	L	8.3	L	45.8	L	25
	R	79.2	R	8.3	R	100	R	8.3	R	37.5	R	33.3
Nerve Lesioned **Week 3**	L	0	L	0	L	37.5	L	0	L	0	L	0
	R	83.3	R	12.5	R	91.7	R	0	R	16.7	R	33.3
Nerve Lesioned **Week 4**	L	0	L	0	L	8.3	L	25	L	0	L	0
	R	100	R	50	R	83.3	R	58.3	R	75	R	62.5
Nerve Lesioned **Week 5**	L	0	L	0	L	25	L	0	L	0	L	0
	R	87.5	R	0	R	91.7	R	33.3	R	66.7	R	62.5
Nerve Lesioned **Week 6**	L	0	L	16.7	L	0	L	0	L	0	L	0
	R	87.5	R	20.8	R	83.3	R	54.2	R	55.6	R	50